Catalysis Today 158 (2010) 258–262

Contents lists available at ScienceDirect

Catalysis Today

journal homepage: www.elsevier.com/locate/cattod

Ni-Ag-O as catalyst for a novel one-step reaction to convert ethane to ethylene oxide

Ying Wu[a,*], Aifeng Yan[a], Yiming He[b], Binfu Wu[a], Tinghua Wu[a,*]

[a] *Laboratory of the Ministry of Education for Advanced Catalysis Materials, Institute of Physical Chemistry, Zhejiang Normal University, Jinhua, 321004, China*
[b] *College of Mathematics, Physics and Information Engineering, Zhejiang Normal University, Jinhua, 321004, China*

ARTICLE INFO

Article history:
Available online 18 April 2010

Keywords:
Ethylene oxide
One-step reaction
Ethane
Interaction

ABSTRACT

The use of a Ni-Ag-O catalyst in a one-step reaction to produce ethylene oxide from ethane was investigated. An optimum ethylene oxide yield of 1.2% was obtained with a selectivity of 12.8% at 310 °C. The catalyst was characterized through X-ray diffraction, BET surface area, H_2 temperature-programmed reduction, O_2 temperature-programmed desorption and X-ray photoelectron spectroscopy. The results showed that NiO and Ag in the catalyst favored ethane activation and the formation of ethylene oxide, respectively.

© 2010 Elsevier B.V. All rights reserved.

1. Introduction

The epoxidation of ethylene (C_2H_4) to ethylene oxide (EO) is an important industrial process [1,2], since EO is a reaction intermediate in the formation of ethylene glycol and polyester fibers [3,4]. EO is most effectively produced over silver supported on low-surface-area α-alumina catalyst by partial oxidation of ethylene with air or oxygen below 300 °C [5,6]. On the other hand, feed ethylene is mainly produced by the thermal pyrolysis of ethane (C_2H_6) or naphtha over 900 °C, a process that operates under severe conditions with high-energy consumption and difficult product separation [7,8]. Hence, it is desirable to design a catalyst over which ethylene oxide could be directly synthesized via a one-step reaction from ethane under mild reaction conditions and without the separation and reuse of ethylene.

To realize a direct conversion of ethane to ethylene oxide, the alternative catalyst should possess dual functions of oxidative dehydrogenation of ethane and epoxidation of ethylene. Many researchers have attempted to replace thermal pyrolysis by catalytic oxidative dehydrogenation (ODH) [9–22]. However, due to the structural stability of ethane, the reaction temperature of the oxidative dehydrogenation of ethane (ODHE) has to exceed 600 °C [10–18]. Although a high ethylene yield could be obtained over some excellent low-temperature catalysts, such as MoVTeNbO, the reaction temperature was not lower than 400 °C [19–21]. For the epoxidation of ethylene to ethylene oxide, however, such a high reaction temperature could easily cause further oxidation of the product to CO_x. Moreover, these low-temperature ODHE catalysts generally complied with the redox (Mars and van Krevelen) mechanism, and its active species is the lattice oxygen [22]. However, research on a suitable Ag catalyst for the epoxidation of ethylene has shown that the appropriate active species should either be molecular or adsorbed atomic oxygen, lattice oxygen is not suitable as it is too active for this reaction [23]. Thus, these ODHE catalysts were unsuitable candidates for use in the design a new bi-functional catalyst. Both reaction temperature and active oxygen species pose limitations on the combination of the two reactions, namely, oxidative dehydrogenation of ethane to ethylene and epoxidation of ethylene to ethylene oxide.

In our previous work, nanosized NiO exhibited appreciable low-temperature catalytic performance for the oxidative dehydrogenation of ethane to ethylene below 300 °C [24]. The adsorbed electrophilic oxygen species was considered as the active species involved in the reaction. This phenomenon is different from the reduction of a transition metal oxide over some other bulk catalysts [25,26]. Thus, it implies that the addition of NiO to Ag might be a possible way to directly convert of ethane to ethylene oxide.

In this study we report a NiO-doped Ag catalyst (Ni-Ag-O), prepared by using a hydrothermal synthesis method. The catalysis of a one-step reaction to convert ethane to ethylene oxide was studied, and the catalysts were characterized by X-ray diffraction (XRD), BET surface area analysis, H_2 temperature-programmed reduction (H_2-TPR), O_2 temperature-programmed desorption (O_2-TPD) and X-ray photoelectron spectroscopy (XPS). This study aims to investigate the catalytic properties of the Ni-Ag-O catalyst in the selective oxidation of ethane and to gain insight into the structural require-

---

* Corresponding authors. Tel.: +86 0579 82283907; fax: +86 0579 82282595.
E-mail addresses: yingwu@zjnu.cn, ying-wu@zjnu.cn (Y. Wu), thwu@zjnu.cn (T. Wu).

0920-5861/$ – see front matter © 2010 Elsevier B.V. All rights reserved.
doi:10.1016/j.cattod.2010.03.041

ments for the conversion of ethane and the formation of selective oxidation products.

2. Experimental

2.1. Catalyst preparation

A series of Ni-Ag-O catalysts was prepared by a hydrothermal synthesis method using $Ni(NO_3)_2\cdot 6H_2O$ and $AgNO_3\cdot 5H_2O$ with different Ni contents (mol ratio of Ni/Ni + Ag). Stoichiometric urea solution was added to the mixture solution of $Ni(NO_3)_2$ and $AgNO_3$. The mixture was transferred into a Teflon-lined stainless steel autoclave, which was subsequently sealed. The samples was aged at 100 °C for 20 h and then cooled to room temperature. The resulting solid was filtered and washed several times with deionized water and absolute ethanol. Finally, it was dried at 110 °C for 10 h, followed by calcination at 400 °C for 4 h in air. For comparison purposes, pure NiO and Ag were prepared using the same method.

2.2. Activity testing

The catalytic test was performed in a fixed-bed vertical-flow tubular quartz reactor (i.d. = 5 mm) packed with 0.1 g catalyst sample. The feed gas consisted of ethane, oxygen, and nitrogen ($C_2H_6/O_2/N_2 = 1/1/6$), with a gaseous hourly space velocity (GHSV) of 24,000 mL h^{-1} g^{-1}. The reactants and products were analyzed using an on-line gas chromatography equipped with a thermal conductivity detector (TCD) attached with a Porapak Q and a 5 Å molecular sieve column.

2.3. Catalyst characterization

The BET surface areas of the samples were determined after degassing the samples at 300 °C and analyzing the N_2 adsorption isotherm at the liquid nitrogen temperature (Tristar 3000). Phase identification and structural analysis were performed by XRD (Model D/Max-C, Rigaku), with a Cu-Kα radiation ($\lambda = 0.15406$ nm) and step scanning (0.02°) in the 2θ range of 20–90°. The average crystalline sizes were calculated from the Scherrer Formula ($D = 0.89\lambda/\beta\cos\theta$). The H_2-TPR experiments were performed on a laboratory-constructed chromatograph using 5% H_2/Ar mixed gas as reduction agent delivered at a flow rate of 17.5 mL/min. The O_2-TPD experiments were conducted on a mass spectrometer (MS) (Balzer Omni Star 200). The catalysts (0.1 g) were first pretreated in air for 0.5 h at 400 °C and then cooled to room temperature. After the system was purged with a He gas flow to smoothen the baseline, the sample was heated to 820 °C under He at a constant rate of 20 °C/min. The samples were analyzed by XPS using a VG ESCALAB/Auger spectrometer to identify the oxidation states of the surface. The effect of charging was corrected by means of adventitious carbon (284.6 eV) referencing.

3. Results and discussion

3.1. Catalytic performance

Table 1
Catalytic performance of the catalysts for the ethane oxidative reaction[a].

Catalyst	Conversion (%)		Selectivity (%)			Yield/% C_2H_4O
	C_2H_6	C_2H_4	C_2H_4O	C_2H_4	CO_2	
NiO	21.6		–	40.8	59.2	–
Ag	–		–	–	–	–
NiO + Ag[b]	18.9		–	7.3	92.7	–
Ni-Ag-O	7.6		14.3	19.8	65.9	1.1
Ag		12.2 [c]	37.4	–	62.6	4.6
NiO + Ag[b]		17.6[c]	–	–	100	–

[a] Reaction conditions: $T = 300$ °C, $O_2:C_2H_6:N_2 = 1:1:6$.
[b] Mixture catalyst of NiO and Ag (Molar ratio Ni:Ag = 1:19).
[c] Reaction temperature: 230 °C.

Before the test, an empty tube loaded with NiO or Ag was evaluated for the partial oxidation of ethane below 350 °C. The pure Ag catalyst showed ethane inactive, based on the reaction data listed in Table 1. Over the NiO catalyst only C_2H_4 and the overoxidation product, CO_2, were obtained, while ethylene oxide was not observed. The physically combined mixture of NiO and Ag exhibited a catalytic behavior similar to the pure NiO catalyst, except that it had lower C_2H_4 selectivity. And the mixed catalyst for the epoxidation of ethylene also did not yield any C_2H_4O. It is obvious that direct conversion of ethane to ethylene oxide could not be realized just by physically mixing NiO and Ag catalysts. Unlike the mixed catalyst, over NiO-doped Ag catalyst (Ni-Ag-O) C_2H_4O was produced along with C_2H_4 and CO_2 as the products of the ethane oxidation reaction.

We prepared a series of Ni-Ag-O catalysts by a hydrothermal synthesis method and investigated their catalytic behavior. Based on the results in Fig. 1, it can be seen that the doping of NiO to Ag catalyst, even a very small amount, could realize the one-step direct conversion of ethane to EO. Increasing the Ni content resulted in a gradual increase of ethane conversion, while C_2H_4O selectivity decreased sharply. The selectivity to EO decreased to nearly zero when the Ni content exceeded 10%. This suggested that NiO in the Ni-Ag-O catalyst was crucial to the activation of ethane, despite its low content. While the Ag in the catalyst was responsible for the epoxidation of ethylene, which might be in the form of an intermediate and could be obtained from the oxidation of ethane on the surface of NiO in the catalyst. The yield of EO reached a maximum at a Ni content of 5%. We also studied the stability of the 5% Ni-Ag-O catalyst. As shown in Fig. 2, ethane conversion and C_2H_4O yield maintained their initial values for the entire 48 h of the experiment, which indicated high catalyst stability. To gain information on the reaction paths for the formation of EO, we investigated in detail the selective oxidation of C_2H_6 over the 5% Ni-Ag-O catalyst.

The effects of the reaction temperature on C_2H_6 conversion and product selectivity over the 5% Ni-Ag-O catalyst are shown in Table 2. It is found that C_2H_6 conversion increased with increasing reaction temperature, while C_2H_4 selectivity decreased. The selectivity to EO increased with an increase in temperature up to 300 °C. Further increases in temperature resulted to a decrease in EO selectivity. When the reaction temperature exceeded 300 °C, both of selectivity to ethylene and EO decreased, while CO_2 selectivity increased. An optimal EO yield of 1.2% was obtained at 310 °C

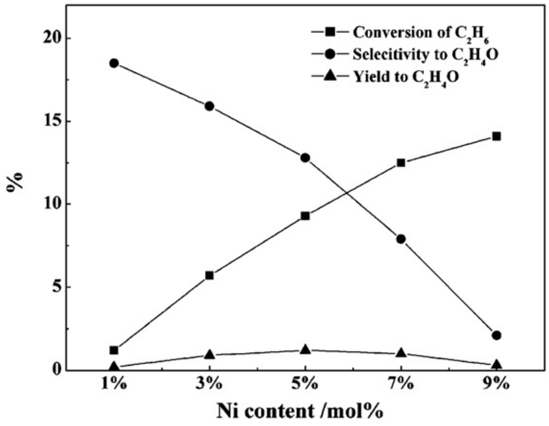

Fig. 1. Dependence of catalytic behaviors of Ni-Ag-O catalysts on Ni content. (Reaction temperature: 310 °C).

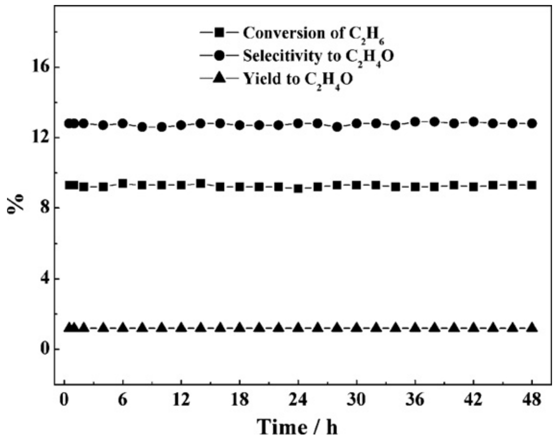

Fig. 2. Stability of 5% Ni-Ag-O catalyst as a function of time on stream. (Reaction conditions: $T = 310\,^{\circ}C$, GHSV = 24,000 mL h^{-1} g^{-1}).

Table 2
Catalytic performance of 5% Ni-Ag-O catalyst with reaction temperature[a].

Temperature (°C)	Conversion (%)	Selectivity (%)		Yield (%)
	C_2H_6	C_2H_4O	C_2H_4	C_2H_4O
250	0.5	0.4	46.4	0.02
270	3.1	4.9	35.8	0.2
290	5.5	10.9	25.3	0.6
300	7.6	14.3	19.8	1.1
310	9.3	12.8	15.6	1.2
320	11.1	8.5	11.3	0.9
340	15.3	2.6	8.2	0.4

[a] Reaction conditions: O_2:C_2H_6:N_2 = 1:1:6, GHSV = 24,000 mL h^{-1} g^{-1}.

with an ethane conversion of 9.3%. This observation may suggest that EO was produced as a secondary product of ethane.

To further clarify this point, we investigated the effect of pseudo-contact time, *W*/*F*, on the catalytic performance of 5% Ni-Ag-O catalyst at 300 °C. The results (listed in Table 3) indicated that a shorter contact time favors the selectivity to C_2H_4, whereas a longer contact time favors the selectivity to C_2H_4O. However, a further increase in contact time (>0.15 s g mL^{-1}) resulted in greater oxidation of EO to CO_2 and a decrease in the selectivity to EO. Thus, EO may likely be produced mainly from the consecutive oxidation of C_2H_4 over the 5% Ni-Ag-O catalyst.

3.2. Structural characteristics

As shown in the XRD patterns (Fig. 3) the broader diffraction peaks of pure NiO sample suggested the existence of a small particle size and large surface area, which are consistent with the calculated result from the Scherrer Formula (7.3 nm) and the surface area data obtained through N_2-sorption measurement (81 m^2/g). A large surface area was possibly beneficial for the activation of ethane, but also contributed to the overoxidation of the product, which was not suitable for the selective oxidation of ethane to EO. The XRD pattern of fresh 5% Ni-Ag-O catalyst only displayed the presence of Ag and not Ni or NiO. This might be due to a low Ni content or/and a high dispersion of NiO in the catalyst. The narrow diffraction peaks indicated its large particle size and small surface area (<1 m^2/g). No change was observed between the phases before and after the catalytic tests.

Table 3
Effect of contact time on the performance of 5% Ni-Ag-O catalyst[a].

W/*F* (s g mL^{-1})	Conversion (%)	Selectivity (%)	
	C_2H_6	C_2H_4O	C_2H_4
0.1125	4.4	9.3	28.5
0.128	5.8	11.7	24.9
0.15	7.6	14.3	19.8
0.18	8.6	13.8	15.1
0.225	9.8	10.9	10.8

[a] Reaction conditions: $T = 300\,^{\circ}C$, O_2:C_2H_6:N_2 = 1:1:6.

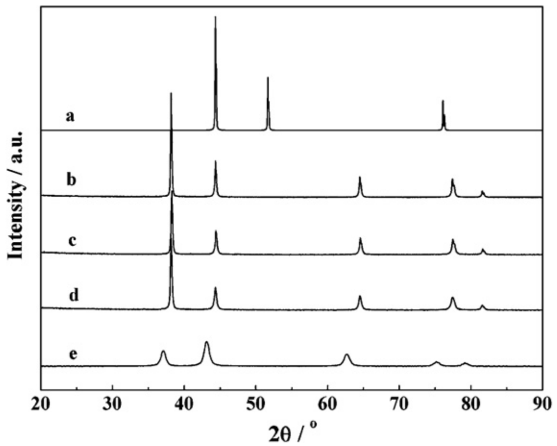

Fig. 3. XRD patterns of (a) Ni, (b) fresh Ni-Ag-O, (c) used Ni-Ag-O, (d) Ag, and (e) NiO.

3.3. H_2-TPR studies

The H_2-TPR profile of pure NiO catalyst (Fig. 4a) showed two main reductions, one for Ni_2O_3 to NiO at 245 °C and the other for NiO to Ni at 418 °C. The shoulder peak at 527 °C might be ascribed to the reduction of NiO with different sizes, whereas the addition of Ag significantly changed the reduction profile (Fig. 4b). A small reduction peak at about 363 °C was observed for the 5% Ni-Ag-O catalyst. Since no reduction peak was observed for the pure Ag and Ni samples (Fig. 4c and d), the only peak of the Ni-Ag-O profile could be ascribed to the reduction of NiO to Ni. The changes in reduction profile and temperature might due to the interaction between NiO and Ag. It can be speculated that NiO was well distributed in the catalyst and had interaction with Ag using a hydrothermal synthesis method through both XRD and TPR characterizations. For the oxidative dehydrogenation of ethane the appearance of metal Ni induced the cleavage of ethane to form methane and hydrogen, with no ethylene selectivity [27,28]. The reducible ability of NiO was retarded due to the addition of Ag, resulting in an enhanced ability to prevent the cleavage of ethane and leading to a high reaction stability.

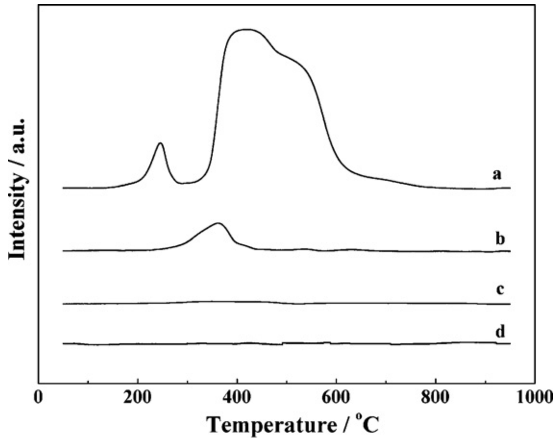

Fig. 4. H_2-TPR profiles of (a) NiO, (b) Ag-Ni-O, (c) Ag, and (d) Ni.

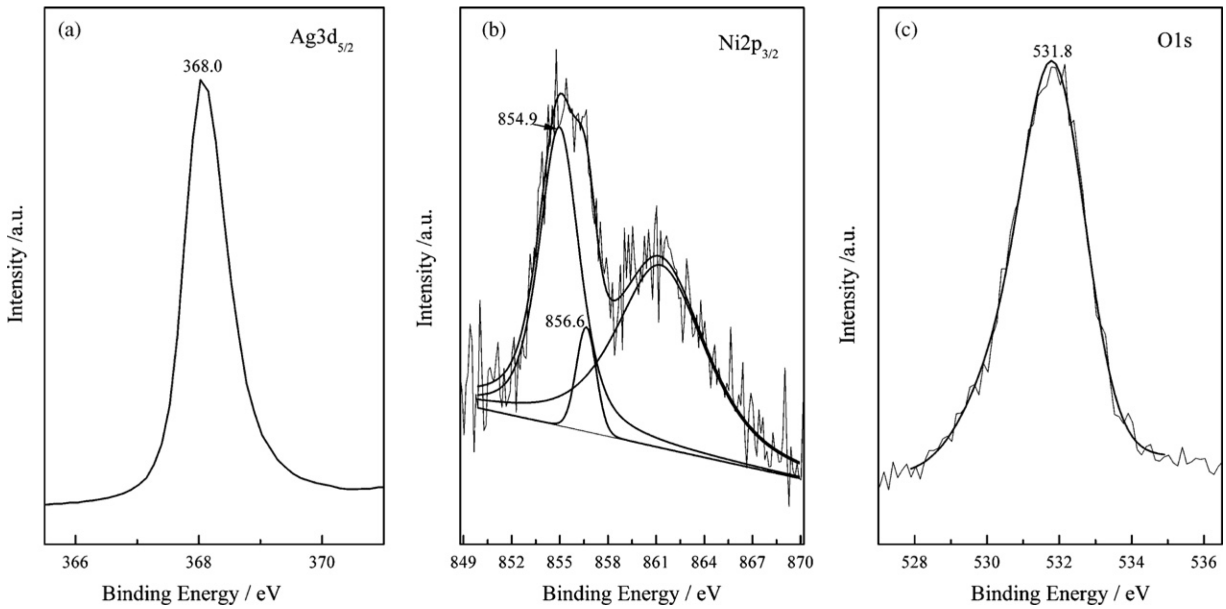

Fig. 5. XPS spectra of (a) Ag $3d_{5/2}$, (b) Ni $2p_{3/2}$, and (c) O 1s.

3.4. XPS studies

To further clarify the interaction between NiO and Ag, samples were analyzed by XPS (Fig. 5). The Ag $3d_{5/2}$ XPS spectrum (Fig. 5a) shows a signal at 368.0 eV with FWHM of 1.0 eV. From the reference spectra of metallic and oxide forms of Ag [29], there was no shift of Ag $3d_{5/2}$ signal between Ag^0 (peak center at 368.0 eV, FWHM of 0.9 eV) and Ag_2O (peak center at 368.0 eV, FWHM of 1.3 eV). However, the bandwidth broadened by 0.4 eV. Therefore, Ag likely remained metallic form and only a few converted to the oxide state on the surface. After NiO was doped in Ag, the binding energy (B.E.) of Ni $2p_{3/2}$ shifted to higher values, from 854.1 and 855.9 eV (Ni^{2+}) to 854.9 and 856.6 eV, respectively. This could be due to its interaction with Ag. The B.E. value was near that of Ni^{3+}. It can be speculated that Ni-Ag-O had more $Ni^{2+\delta}$ contents, thus rendering its B.E. closer to that of Ni_2O_3. The shift of O 1s B.E. (Fig. 5c) from 530.1 eV (NiO) to 531.8 eV also suggested the existence of a higher valance $Ni^{2+\delta}$ [30–32] in 5% Ni-Ag-O catalyst.

Although only the peaks of Ag were detected in the XRD patterns for 5% Ni-Ag-O catalyst, the XPS results clearly indicate that the chemical valence of Ni on the surface had distinct variation compared with that of pure NiO. Thus, based on the changed reduction of the Ni-Ag-O catalyst and the valence variation of NiO on the surface, it can be deduced that there was an interaction between Ag and NiO.

3.5. Raman studies

Fig. 6 shows the Raman spectra of the catalysts. The figure illustrates that the Ag catalyst exhibited bands at ca. 552, 802, 914 cm^{-1}, which was attributed to the Ag-O vibration since Ag alone was Raman-inactive [33]. The spectrum of NiO exhibited a broad band centered at 525 cm^{-1}, which is associated with Ni-O skeletal vibration [34]. For the Ni-Ag-O catalyst, aside from the bands of Ag and NiO, four new peaks were observed at around 375, 456, 685 and 987 cm^{-1}, which should be related to the vibration of Ag-O-Ni. Raman results further indicated the existence of an interaction between Ag and NiO. In addition, the appearance of signals for Ag-O-Ni suggested that the Ni-O site was isolated by Ag, which may have some influence on the catalytic performance.

3.6. O_2-TPD-MS studies

The O_2-TPD-MS performance of 5% Ni-Ag-O catalyst is shown in Fig. 7. For comparison, the desorption profiles of NiO and Ag are also been shown. The NiO profile exhibited a large oxygen desorption peak in the 350–600 °C range, with a maximum temperature of desorption at about 450 °C. The Ag profile exhibited a small oxygen desorption at about 600–800 °C. From the results of the reaction performance results, it was observed that pure Ag catalyst showed ethane inactive below 350 °C, but at the reaction temperature range ethylene could be epoxidized to EO over the Ag catalyst. Based on the reaction data, it is known that the catalyst on the basis of Ag was effective for converting ethylene to EO. Thus, it could be suggested that high-temperature desorption oxygen might have been favorable for the epoxidation of ethylene and could be considered as the epoxidative active species for the C=C double bond. However, this type of adsorbed electrophilic oxygen species could not activate the C–H bond of ethane. On the other hand, the oxygen species from low-temperature desorption on the NiO catalyst surface exhibited higher catalytic activity and was advantageous for activating ethane. The Ag catalyst was not suitable for activating ethane due to the small amount of low-temperature adsorbed oxygen. For NiO catalyst, however, its large low-temperature des-

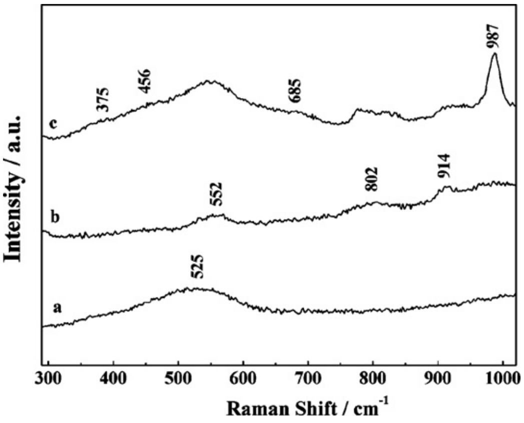

Fig. 6. Raman spectra of (a) NiO, (b) Ag, and (c) Ni-Ag-O.

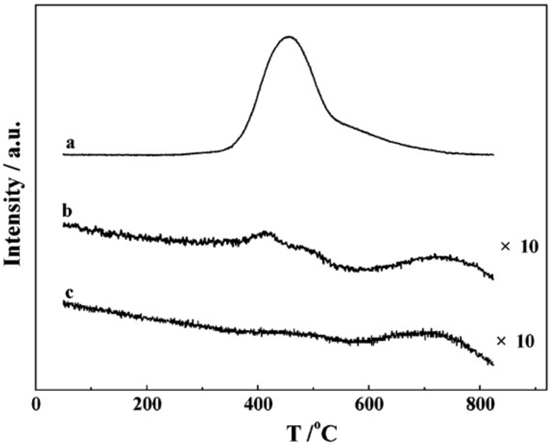

Fig. 7. O_2-TPD-MS profiles of (a) NiO, (b) Ni-Ag-O, and (c) Ag.

orption oxygen peak suggested a higher catalytic activity of ethane to ethylene and even to the overoxidation product, CO_2. Using physically combined mixture of NiO and Ag catalysts could yield ethylene as an intermediate of the oxidative dehydrogenation of ethane on the NiO surface site. The rapid consecutive oxidation of C_2H_4 to C_2H_4O over the Ag catalyst may be responsible for its lower selectivity to ethylene. In a short time the small quantity of C_2H_4O could be deeply oxidized into the overoxidation CO_2 over active NiO catalyst with a large surface area. When NiO was doped in Ag, there was an obvious variety of oxygen adsorption due to the interaction of NiO and Ag. Meanwhile, the small amount of high-temperature oxygen species could epoxidize intermediate ethylene to ethylene oxide.

Due to the doping of NiO, low-temperature oxygen species could be adsorbed on the Ni-Ag-O catalyst surface, and this could activate ethane at a lower reaction temperature. On the other hand, the addition of Ag restrained the surface area of the catalyst. Thus, the low-temperature oxygen species on the catalyst surface decreased sharply, which led to a decrease in catalytic activity. At the same time, because of the existence of Ag-O-Ni, the ethylene produced on the Ni-O surface could continue to be epoxidized to EO on an adjacent Ag surface site. However, compared with the physically combined NiO and Ag catalyst, the overoxidation of the target product, EO, through active low-temperature oxygen species on the Ni-O surface was inhibited to a certain degree due to the isolation of the Ni-O active site by Ag.

4. Conclusions

In summary, EO could be directly synthesized from ethane over the Ni-Ag-O catalyst prepared by hydrothermal method, with ethylene as an intermediate. The decreased reduction of NiO in the catalyst and the variety of chemical values on the catalyst surface suggested that there was an interaction between NiO and Ag, which resulted in the separation of the active sites and the variety of adsorption performance. The low-temperature adsorbed oxygen species on the NiO surface was related to ethane activity, and the high-temperature oxygen species on the Ag surface contributed to the formation of EO. Thus EO can be produced directly by conversion of ethane over the Ni-Ag-O catalyst possibly because the catalyst possessed both types of adsorbed oxygen species. At present although the EO yield is low, the novel one-step reaction and relevant active catalyst still proved interesting and worthwhile for further research.

Acknowledgements

This work is supported by grants from the Natural Science Foundation of Zhejiang Province in China (Y406322) and Science and Technology Ministry of Zhejiang Province (2009C31084).

References

[1] N. Macleod, J.M. Keel, R.M. Lambert, Catal. Lett. 86 (2003) 51.
[2] E.A. Carter, W.A. Goddard, J. Catal. 112 (1988) 80.
[3] M.C.J. Bradford, D.X. Fuentes, Catal. Commun. 3 (2002) 51.
[4] Y. Kim, N. Park, J. Shin, S.R. Lee, Y.J. Lee, D.J. Moon, Catal. Today 87 (2003) 153.
[5] D. Torres, N. Lopez, F. Illas, J. Catal. 243 (2006) 404.
[6] Y. Ayame, H. Uchida, M. Ono, T. Miyamoto, H. Sato, Hayasaka, Appl. Catal. A: Gen. 244 (2003) 59.
[7] E. Heracleous, A.A. Lemonidou, Appl. Catal. A: Gen. 269 (2004) 123.
[8] S.A.R. Mulla, O.V. Buyevskaya, M. Baerns, Appl. Catal. A: Gen. 226 (2002) 73.
[9] E.M. Thorsteinson, T.P. Wilson, F.G. Young, P.H. Kasai, J. Catal. 52 (1978) 116.
[10] L. Ji, J. Liu, C. Liu, X. Chen, Appl. Catal. A 114 (1994) 207.
[11] O. Desponds, R.L. Keiski, G.A. Somorjai, Catal. Lett. 19 (1993) 17.
[12] E.M. Kennedy, N.W. Cant, Appl. Catal. A 87 (1992) 171.
[13] E. Reverchon, G.D. Porta, et al., Stud. Surf. Sci. Catal. 118 (1998) 349.
[14] D.J. Wang, M.P. Rosynek, J.H. Lunsford, J. Catal. 151 (1995) 155.
[15] C.T. Au, K.D. Chen, H.X. Dai, Y.W. Liu, J.Z. Luo, C.F. Ng, J. Catal. 179 (1998) 300.
[16] D.W. Flick, M.C. Huff, J. Catal. 178 (1998) 315.
[17] Y. Liu, Y. Zhang, X. Liu, J. Xue, S. Li, Chem. Lett. 27 (1998) 1057.
[18] S.B. Wang, K. Murata, T. Hayakawa, S. Gamakawa, K. Suzuki, Chem. Commun. (1999) 103.
[19] E. Heracleous, A.A. Lemonidou, J. Catal. 237 (2006) 162.
[20] J.M.L. Nieto, P. Botella, M.I. Vázquez, A. Dejoz, Chem. Commun. (2002) 1906.
[21] P. Botella, E. García-González, A. Dejoz, J.M. López Nieto, M.I. Vázquez, J. González-Calbet, J. Catal. 225 (2004) 428.
[22] X. Li, E. Iglesia, Appl. Catal. A: Gen. 334 (2008) 339.
[23] T. Jomoto, J. Lin, T. Nakajima, J. Mol. Struct. (Theochem.) 577 (2002) 143.
[24] Y. Wu, Y. He, T. Wu, W. Weng, H. Wan, Mater. Lett. 61 (2007) 2679.
[25] X. Zhang, Y. Gong, G. Yu, Y.C. Xie, J. Mol. Catal. A: Chem. 180 (2002) 293.
[26] Y. Schuurman, V. Ducarme, T. Chen, W. Li, C. Mirodatos, G.A. Martin, Appl. Catal. A: Gen. 163 (1997) 227.
[27] T. Chen, W.Z. Li, C.Y. Yu, R.C. Jin, H.Y. Xu, Stud. Surf. Sci. Catal. 130B (2000) 1847.
[28] T. Chen, W.Z. Li, C.Y. Yu, Chin. J. Catal. 19 (1) (1998) 37.
[29] R.N. Lamb, B. Ngamsom, D.L. Trimm, B. Gong, P.L. Silveston, P. Praserthdam, Appl. Catal. A: Gen. 268 (2004) 43.
[30] A.F. Carley, S.D. Jackson, M.W. Roberts, J. O'Shea, Surf. Sci. 454 (2000) 141.
[31] C.N.R. Rao, V. Vijayakrishnan, G.U. Kulkarni, M.K. Rajumon, Appl. Surf. Sci. 84 (1995) 285.
[32] M.S. Hedge, M. Ayyoob, Surf. Sci. 173 (1986) L635.
[33] G.I.N. Waterhouse, G.A. Bowmaker, J.B. Metson, Appl. Surf. Sci. 214 (2003) 36.
[34] T. Chen, Y.C. Shen, Y. Wu, M.G. Jin, W.Z. Weng, H.L. Wan, Chin. J. Light Scatt. 14 (2002) 72.